

C-Terminus of Botulinum A Protease Has Profound and Unanticipated Kinetic Consequences upon the Catalytic Cleft

Peter Šilhár,[†] Matthew A. Lardy,[‡] Mark S. Hixon,[‡] Charles B. Shoemaker,[§] Joseph T. Barbieri,^{||} Anjali K. Struss,[†] Jenny M. Lively,[†] Sacha Javor,[†] and Kim D. Janda^{*,†,⊥}

[†]Departments of Chemistry and Immunology, and The Skaggs Institute for Chemical Biology, The Scripps Research Institute, 10550 North Torrey Pines Road, La Jolla, California 92037, United States

[‡]Takeda California Inc., 10410 Science Center Drive, San Diego, California 92121, United States

[§]Department of Biomedical Sciences, Tufts Cummings School of Veterinary Medicine, 200 Westboro Road, North Grafton, Massachusetts 01536, United States

^{||}Department of Microbiology and Molecular Genetics, Medical College of Wisconsin, 8701 Watertown Plank Road, Milwaukee, Wisconsin 53226, United States

[⊥]Worm Institute for Research and Medicine (WIRM), The Scripps Research Institute, 10550 North Torrey Pines Road, La Jolla, California 92037, United States

S Supporting Information

ABSTRACT: Botulinum neurotoxins (BoNTs) are among the most deadly poisons known, though ironically, they also are of great therapeutic utility. A number of research programs have been initiated to discover small molecule inhibitors of BoNTs metalloprotease activity. Many, though not all, of these programs have screened against a truncated and more stable form of the enzyme, that possesses comparable catalytic properties to the full length enzyme. Interestingly, several classes of inhibitors, notably the hydroxamates, display a large shift in potency between the two enzyme forms. In this report we compare the kinetics of active-site, α -exosite and β -exosite inhibitors versus truncated and full length enzyme. Molecular dynamics simulations conducted with the truncated and homology models of the full length BoNT LC/A indicate the flexibility of the C-terminus of the full length enzyme is responsible for the potency shifts of active-site proximally binding inhibitors while distal binding (α -exosite) inhibitors remain equipotent.



KEYWORDS: Botulinum neurotoxin, zinc-dependent metalloprotease, protease inhibitor, small molecule inhibitor, natural product

Botulinum neurotoxins (BoNTs), of which there are seven serotypes, A–G,¹ are proteins produced by bacteria of the genus *Clostridium*.² Botulism, although rare, is serious, since BoNTs are the most poisonous substances known, with serotype A having a lethal dose for a 70 kg human of approximately 0.09–0.15 μg intravenously or intramuscularly, and 0.7–0.9 μg inhalationally.³ Despite their potentially lethal toxicity, BoNTs have emerged as extremely valuable therapeutic tools for the treatment of a variety of maladies, including strabismus, migraines, and even facial wrinkles.^{4,5} However, the potential misuse of BoNT in a bioterrorist attack remains imminent and the Center for Disease Control (CDC) now classifies this agent as “category A”, placing it among the six highest-priority agents. Current treatments for botulinum poisoning are all antibody-based with a limited window of therapeutic effectiveness.⁶

Inhibition of the BoNT light chain metalloprotease is a logical therapeutic strategy for the treatment of botulism, since it will provide an effective postexposure remedy. In these

regards, BoNTs are synthesized as 150 kDa proteins that are post-translationally activated by proteolytic cleavage to form mature dichain proteins consisting of a 100 kDa heavy chain (HC) and a 50 kDa light chain (LC) linked by a disulfide bond.⁷ The HC is responsible for neurospecific cellular binding, uptake, and translocation of the LC into the cytosol of neuronal cells. The LC is a Zn^{2+} -dependent metalloprotease that cleaves one of three intracellular soluble N-ethylmaleimide-sensitive factor attachment protein receptor (SNARE) proteins: syntaxin, vesicle-associated membrane protein (VAMP)/synaptobrevin, or synaptosomal-associated protein of 25 kDa (SNAP-25), depending on the serotype. As a consequence of protein cleavage, release of acetylcholine at the neuromuscular junction is blunted, resulting in the loss of neurotransmission.

Received: November 29, 2012

Accepted: December 22, 2012

Published: December 23, 2012

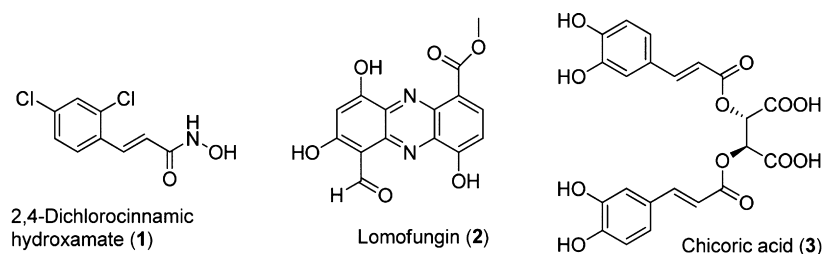


Figure 1. Structures of re-evaluated BoNT/A LC inhibitors.

Working with the native full length LC of BoNT/A is challenging. Pioneering research has demonstrated that full length LC of BoNT/A suffers from catalytic fragmentation.^{8,9} Smith and co-workers have extensively explored and reported on this limited stability of the BoNT/A LC.^{10–12} They determined that this truncation/fragmentation process is autocatalytic and have identified several cleavage sites.¹⁰ Apart from autocatalytic truncation/fragmentation of the full length BoNT/A LC, there are several other liabilities associated with this protease form, including poor solubility and dimer formation mediated by Cys430.¹³ To surmount these obstacles, Barbieri et al. have prepared and evaluated several BoNT/A LC constructs with C-terminal truncations in order to increase solubility as well as stability.¹³ This research suggested that the LC 1–425 construct behaved optimally, exhibiting better solubility and stability with substrate specificity constants ($k_{\text{cat}}/K_{\text{M}}$) comparable with those of the natural full length LC 1–448.

Engaging a truncated enzyme form that possesses enhanced *in vitro* stability is a common practice in drug discovery campaigns. For example, receptor tyrosine kinases (RTKs) are typically truncated to the catalytic domain.¹⁴ Occasionally though, the potency of inhibitors may differ substantially between the truncated form and a more extended form. When binding discrepancies are observed between truncated and extended enzyme forms, these usually result from disordered or flexible loops of high mobility.

We have embarked on a program to identify a spectrum of new small-molecule inhibitors of BoNTs, some of which engage the catalytic residues while others bind distal to the catalytic core yet still inhibit catalysis.^{6,15,16} By use of rational drug design and high throughput screening, our group has discovered and reported several potent and mechanistically distinct small molecule inhibitors of BoNT/A LC (Figure 1), e.g. 2,4-dichlorocinnamic hydroxamate (1),¹⁶ D-chicoric acid (3),¹⁷ and Lomofungin (2).¹⁸ Disappointingly, these molecules provide only modest activity in both cell based and animal studies. We thus questioned if differences between truncated and full length forms of the protease may contribute to the lack of cellular potency. Herein, we disclose an in depth examination of inhibitor binding by empirical methods as well as by molecular dynamics. The research described gives insight into the important problematic issue of LC differences observed with previously characterized inhibitors of BoNT/A.

As a starting point we analyzed the kinetic parameters of both the full length and truncated proteases. Enzyme catalytic activity was determined by use of an LC/MS-based assay,¹⁹ making use of a truncated SNAP-25 (141–206) peptide substrate, encompassing the key recognition elements of SNAP-25 (see Supporting Information for details). It is important to note that this 66-mer cored out from native SNAP-25 (141–206) has no structural modification; thus, the

integrity of the protein substrate molecule is not compromised and potential kinetic complications seen with incorporated modified fluorescent labels are eliminated.²⁰ As anticipated, the k_{cat} and K_{M} values for both the full length and truncated proteases were comparable (Table 1).

Table 1. Kinetic Parameters for BoNT/A Proteases with 66-mer SNAP-25 Substrate (141–206)

protease	K_{M} (μM)	k_{cat} (s^{-1})	$k_{\text{cat}}/K_{\text{M}}$ ($\text{s}^{-1} \mu\text{M}^{-1}$)
LC 1–448	15 ± 2	6.7 ± 0.4	0.447
LC 1–425 ^a	9 ± 2	2.9 ± 0.2	0.322

^aAlthough lower k_{cat} was reported previously,¹⁵ the current value was obtained with a fresh preparation of the protease.

Three inhibitors with distinct mechanisms of action^{16,17,18} were examined against the truncated form of BoNT/A LC and the extended form, i.e. full length BoNT/A LC (1–448). The inhibitory mechanistic classes are as follows: an active site binder, an α -exosite binder, and a β -exosite binder, thus casting a wide net to probe for protease kinetic differences. The inhibition constants, K_{I} , were determined by a nonlinear least-squares global fit of an appropriate inhibition model to the initial rates of product formation from matrices of substrate–inhibitor concentrations bracketing K_{M} and K_{I} , respectively (Table 2).

Table 2. Comparison of K_{I} Values Determined against Truncated (1–425) and Full Length (1–448) BoNT/A LC

inhibitor	BoNT/A LC (1–425)	BoNT/A LC (1–448)
hydroxamate (1) ^a	$K_{\text{is}} = 0.3 \pm 0.01 \mu\text{M}$ competitive	$K_{\text{is}} = 5.6 \pm 0.8 \mu\text{M}$ competitive
lomofungin (2) ^b	$K_{\text{is}} = 6.7 \pm 0.7 \mu\text{M}$ $K_{\text{ii}} = 6.7 \pm 0.7 \mu\text{M}$ noncompetitive	$K_{\text{is}} = 25 \pm 5 \mu\text{M}$ competitive
D-chicoric acid (3) ^c	$K_{\text{is}} = 0.7 \pm 0.1 \mu\text{M}$ $K_{\text{ii}} = 1.6 \pm 0.3 \mu\text{M}$ noncompetitive	$K_{\text{is}} = 1.4 \pm 0.3 \mu\text{M}$ $K_{\text{ii}} = 3.9 \pm 1.2 \mu\text{M}$ noncompetitive
	partial inhibition	partial inhibition

^aActive site inhibitor. ^b β -exosite inhibitor. ^c α -Exosite inhibitor, K_{is} = competitive inhibition constant, K_{ii} = uncompetitive inhibition constant.

The compounds in Table 2 were divided into two target classes based upon binding location. They were grouped first as active site or exosite inhibitors and second as catalytic or noncatalytic cleft inhibitors. We designated catalytic cleft inhibitors as molecules that bind in both an active site and a β -exosite, since the β -exosite is in apparent close proximity to the catalytic cleft.²¹ By contrast, molecules binding in alternative locations, i.e. an α -exosite, were binned as

noncatalytic cleft inhibitors. On the basis of this nomenclature, hydroxamate **1** coordinates with the active site zinc of the LC 1–425,²² exerting competitive inhibition.¹⁶ Alternatively, kinetic studies reported previously indicate that Lomofungin¹⁸ and chicoric acid¹⁷ bind within exosites on the truncated protease. On the basis of our previous kinetic analysis, lomofungin maps closer to the β -exosite on the protease while chicoric acid would map closer to the α -exosite.²³

Having established the same catalytic kinetic parameters for both LC 1–425 and LC 1–448 with a 66-mer of the native SNAP-25 substrate (Table 1), we were taken aback by discrepancies in activities of some of the inhibitors when tested against these protease forms. Particularly intriguing were the large differences in potencies seen for 2,4-dichlorocinnamic hydroxamate (**1**), especially since this molecule has been crystallized within the active site of the LC 1–425 protease and its binding appears straightforward. The competitive inhibition constant for **1** against LC 1–425 shifts from $0.3 \pm 0.01 \mu\text{M}$ to $K_1 = 5.6 \pm 0.8 \mu\text{M}$ (19-fold upward shift) versus LC 1–448 (Table 2). In contrast, α -exosite binder chicoric acid's K_1 values and inhibition mechanism were virtually identical against both LCs (Table 2). Unexpectedly, lomofungin, our β -exosite binder, presented not only a higher IC_{50} against full length enzyme (9-fold, data not shown) but also a different kinetic mechanism of inhibition. Our molecular modeling studies offer an explanation for the shift in potency of active site proximal binding inhibitors versus active site distal binders.

Three structures of BoNT/A LC (PDB codes: 2ILP, 2IMA, and 2IMB)²² were used for computational modeling. All water molecules were removed using PyMol, and hydrogen atoms were added using Reduce.^{24,25} Each ligand was excised for use in simulations. No additional preparation was necessary, as the coordinates of these systems are from crystal structures.

No crystal structure of full length BoNT/A is currently available. Additionally, the full length enzyme contains a highly mobile loop, presenting a challenge for molecular modeling. To investigate the impact of the additional residues within full length BoNT/A LC (Figure 2), the extra residues were added via homology modeling using Moe.²⁶ The full length FASTA sequence was used with the representative PDB as the template for each homology model created. Zinc and the ligands were treated as environmental atoms and were moved into the

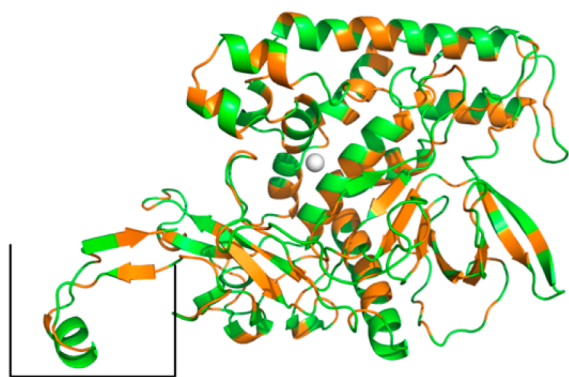


Figure 2. 2IMB structure of BoNT/A LC with the extra residues of the full length modeled in. The residues are colored by hydrophobicity, with hydrophobic residues colored orange and hydrophilic residues colored green. These extra 23 residues in the full length sequence, shown in the lower left corner, are mostly hydrophilic (highlighted in the box).

coordinate system of the best scoring homology model. This was done to ensure that the metal and inhibitor are in the same position with respect to the rest of the system.

We took a conventional approach using Amber11 to simulate complexes.²⁷ Amber99SB and GAFF force fields were used to parametrize the protein and ligand, respectively.^{26,28} Ligands were charged with AM1BCC charges from Firefly.²⁹ Complexes were minimized with 500 steps of minimization in the generalized Born solvent model, followed by a restrained minimization of the system for 200 steps.^{30–32} Following minimization, 30 ps of equilibration were run followed by 5 ns of production simulation. RMSF (root mean square fluctuation) calculations were performed in Gromacs 4.5.5, using trajectories converted by VMD. The RMSF values were placed into the *b*-factor column of the final PDB, and the resulting trajectories were then false colored by *b*-factor.

Molecular dynamics simulations were performed using the crystallographic coordinates of BoNT/A LC and homology modeled systems. In the simulations, the active site zinc chelating inhibitor displayed a consistent difference in binding free energy between the full and truncated sequences (Table 3).

Table 3. Binding Energies of Inhibitors from GBSA Calculations in Amber11

entry	structure ^a (length) ^b	ΔG_{bind} (kcal/mol)	std dev	$\Delta\Delta G_{\text{bind}}$ (kcal/mol)
1	2ILP (1–448)	–26.22	0.56	4.93
	2ILP (1–425)	–31.15	0.32	
2	2IMB (1–448)	–28.36	0.50	11.13
	2IMB (1–425)	–39.49	0.50	
3	2IMA (1–448)	–41.24	0.39	3.95
	2IMA (1–425)	–45.19	0.37	

^aStructure of BoNT/A LC cocrystallized with an inhibitor (2ILP, 4-chlorocinnamic hydroxamate; 2IMB, arginine hydroxamate; 2IMA, 2,4-dichlorocinnamic hydroxamate); see www.pdb.org. ^bBoNT/A LC length.

The molecular modeling results confirmed our empirical observations that the binding affinities of ligands in the active site of full length LC are lower than those for truncated LC.

We questioned lomofungin's inhibitory behavior between protease forms. Lomofungin presented a 9-fold loss of potency against full length enzyme. Additionally, the kinetic mechanism of inhibition changes from classical noncompetitive (truncated) to competitive (full length). Lomofungin is presumed to bind to the β -exosite, which is located within the 250 loop of BoNT/A protease, a region encompassing residues 242–259.²¹ It has been discussed,²² and our molecular modeling studies confirmed, that conformational changes in 250 loop between LC 1–425 and LC 1–448 were pronounced. We consider this altered inhibition pattern of lomofungin as a proof of the different molecular space encompassing the β -exosite between the two enzyme forms. Likely, LC 1–425 contains chemical space for the simultaneous binding of both substrate and lomofungin, whereas in LC 1–448 this is impossible due to a different mobility of the 250 loop. We conservatively consider that Table 3 provides good evidence that the extended C-terminus of LC 1–448 has an influence on binding properties of both active site and β -exosite inhibitors. In contrast, the α -exosite, which is located on the opposite face of the protease, is affected negligibly.

When the trajectories of the full and truncated systems are examined, it appears that the conformational flexibility of the BoNT/A LC explains the observed variations in inhibitory strength. In simulations, the mobility of the extra 23 residues translates into a more mobile core. Therefore, full length LC possesses additional loop mobility near the active site (Figure 3). This is much more impactful on inhibitors that bind within



Figure 3. Homology model of full length 2ILP BoNT/A LC false colored by RMSF. Green sections denote regions that are more mobile than the magenta colored sections. The cocrystallized ligand and the zinc are provided as a reference to orient the structure.

the catalytic cleft versus distally. We propose that it is this additional motility that leads to a reduction in free energies of binding and consequently in lower potency of catalytic cleft inhibitors against full length protease. Substrate binding may be much less affected, since large substrates contain a much larger binding interface area.²¹

Addressing a number of conundrums that have plagued the botulinum neurotoxin field in advancing a therapeutic forward, we have taken a heuristic approach, looking first at the issues regarding two of the most popular constructs of the BoNT/A protease used in both compound selection and mechanistic investigations. Steady-state kinetic analysis clearly shows that both forms of the protease have comparable specificity constants toward substrates. However, inhibitor data, while sparse between both forms of the proteases, has appeared at times conflicting. We have examined classes of inhibitors against two different molecular constructs of the protease to unravel the disparate results seen between enzymatic, cellular, and animal data, as reported by several different groups.³³

To conclude, we chose an active site zinc-chelator, an α -exosite, and a β -exosite inhibitor represented by hydroxamate **1**, chicoric acid **3**, and lomofungin **2**, respectively (Figure 1). We have determined and compared their kinetic inhibition mechanisms against the full length and truncated forms of the protease. Comparison of these data (Table 2) for both LCs (1-425 and 1-448) revealed a significant influence of the extended C-terminus on binding properties of inhibitors in the catalytic cleft. Namely, the active site inhibitor **1** exerts 19-fold lower potency against LC 1-448 when compared with LC 1-425. Similarly, lomofungin, a putative β -exosite inhibitor that binds within the catalytic cleft, displayed 9-fold lower IC_{50} value, and surprisingly, its kinetic inhibition mechanism changed from noncompetitive inhibition to competitive inhibition. In contrast, the potency of chicoric acid (α -exosite inhibitor) remained practically unchanged against both enzyme forms. To try and understand these differences, we have

engaged molecular modeling studies. Using this tool we have demonstrated, on the basis of GBSA simulations, that the residues residing at the C-terminus of full length BoNT/A protease place additional flexibility on the loops surrounding the active site, and it is likely this additional motility that affects the binding capabilities of catalytic cleft inhibitors. In summary, our data present both new insights into BoNT/A protease forms used for inhibitor selection and discrepancies seen in the past literature reports. Lastly, we highlight, it still remains shrouded what form of the LC exists in the cytosol during the SNAP-25 proteolysis, and this ultimately will need resolution for further advancement of the field.^{11,33–35}

■ ASSOCIATED CONTENT

📄 Supporting Information

Biological assay conditions and selected inhibition profiles of compounds **1**, **2**, and **3**. This material is available free of charge via the Internet at <http://pubs.acs.org>.

■ AUTHOR INFORMATION

Corresponding Author

*E-mail: kdjanda@scripps.edu.

Author Contributions

All authors contributed to the Experimental design. J.L. also contributed to the data analysis. P.S., M.L., M.H., A.S., S.J., and K.J. also contributed to both the data analysis and manuscript preparation.

Funding

The authors gratefully acknowledge support of this project by the National Institute of Allergy and Infectious Diseases, National Institute of Health, and the Department of Health and Human Services under Contract Numbers N01-AI30050 and AI080671.

Notes

The authors declare no competing financial interest.

■ REFERENCES

- (1) Schiavo, G.; Matteoli, M.; Montecucco, C. Neurotoxins affecting neuroexocytosis. *Physiol.Rev.* **2000**, *80* (2), 717–66.
- (2) Johnson, E. A.; Bradshaw, M. Clostridium botulinum and its neurotoxins: a metabolic and cellular perspective. *Toxicon* **2001**, *39* (11), 1703–1722.
- (3) Arnon, S. S.; Schechter, R.; Inglesby, T. V.; Henderson, D. A.; Bartlett, J. G.; Ascher, M. S.; Eitzen, E.; Fine, A. D.; Hauer, J.; Layton, M.; Lillibridge, S.; Osterholm, M. T.; O'Toole, T.; Parker, G.; Perl, T. M.; Russell, P. K.; Swerdlow, D. L.; Tonat, K. Botulinum toxin as a biological weapon: Medical and public health management. *JAMA, J. Am. Med. Assoc.* **2001**, *285* (8), 1059–1070.
- (4) Hackett, R.; Kam, P. C. Botulinum toxin: pharmacology and clinical developments: a literature review. *Med. Chem.* **2007**, *3* (4), 333–45.
- (5) Truong, D. D.; Jost, W. H. Botulinum toxin: clinical use. *Parkinsonism Relat. Disord.* **2006**, *12* (6), 331–55.
- (6) Willis, B.; Eubanks, L. M.; Dickerson, T. J.; Janda, K. D. The Strange Case of the Botulinum Neurotoxin: Using Chemistry and Biology to Modulate the Most Deadly Poison. *Angew. Chem., Int. Ed.* **2008**, *47* (44), 8360–8379.
- (7) Oguma, K.; Fujinaga, Y.; Inoue, K. Structure and function of Clostridium botulinum toxins. *Microbiol. Immunol.* **1995**, *39* (3), 161–8.
- (8) Dasgupta, B. R.; Foley, J., Jr.; Botulinum, C. Neurotoxin types A and E: isolated light chain breaks down into two fragments. Comparison of their amino acid sequences with tetanus neurotoxin. *Biochimie* **1989**, *71* (11–12), 1193–1200.

- (9) Ahmed, S. A.; Smith, L. A. Light chain of botulinum A neurotoxin expressed as an inclusion body from a synthetic gene is catalytically and functionally active. *J. Protein Chem.* **2000**, *19* (6), 475–87.
- (10) Ahmed, S. A.; Byrne, M.; Jensen, M.; Hines, H.; Brueggemann, E.; Smith, L. Enzymatic Autocatalysis of Botulinum A Neurotoxin Light Chain. *J. Protein Chem.* **2001**, *20* (3), 221–231.
- (11) Ahmed, S. A.; McPhie, P.; Smith, L. A. Autocatalytically Fragmented Light Chain of Botulinum A Neurotoxin Is Enzymatically Active. *Biochemistry* **2003**, *42* (43), 12539–12549.
- (12) Ahmed, S. A.; Ludivico, M. L.; Smith, L. A. Factors affecting autocatalysis of botulinum A neurotoxin light chain. *Protein J.* **2004**, *23* (7), 445–51.
- (13) Baldwin, M. R.; Bradshaw, M.; Johnson, E. A.; Barbieri, J. T. The C-terminus of botulinum neurotoxin type A light chain contributes to solubility, catalysis, and stability. *Protein Expression Purif.* **2004**, *37* (1), 187–195.
- (14) Schwartz, P. A.; Murray, B. W. Protein kinase biochemistry and drug discovery. *Bioorg. Chem.* **2011**, *39* (5–6), 192–210.
- (15) Boldt, G. E.; Kennedy, J. P.; Hixon, M. S.; McAllister, L. A.; Barbieri, J. T.; Tzipori, S.; Janda, K. D. Synthesis, characterization and development of a high-throughput methodology for the discovery of botulinum neurotoxin a inhibitors. *J. Comb. Chem.* **2006**, *8* (4), 513–21.
- (16) Boldt, G. E.; Kennedy, J. P.; Janda, K. D. Identification of a potent botulinum neurotoxin a protease inhibitor using in situ lead identification chemistry. *Org. Lett.* **2006**, *8* (8), 1729–32.
- (17) Šilhár, P.; Čapková, K. i.; Salzameda, N. T.; Barbieri, J. T.; Hixon, M. S.; Janda, K. D. Botulinum Neurotoxin A Protease: Discovery of Natural Product Exosite Inhibitors. *J. Am. Chem. Soc.* **2010**, *132* (9), 2868–2869.
- (18) Eubanks, L. M.; Šilhár, P.; Salzameda, N. T.; Zakhari, J. S.; Xiaochuan, F.; Barbieri, J. T.; Shoemaker, C. B.; Hixon, M. S.; Janda, K. D. Identification of a Natural Product Antagonist against the Botulinum Neurotoxin Light Chain Protease. *ACS Med. Chem. Lett.* **2010**, *1* (6), 268–272.
- (19) Čapková, K.; Hixon, M. S.; McAllister, L. A.; Janda, K. D. Toward the discovery of potent inhibitors of botulinum neurotoxin A: development of a robust LC MS based assay operational from low to subnanomolar enzyme concentrations. *Chem. Commun.* **2008**, *30*, 3525–3527.
- (20) Pires-Alves, M.; Ho, M.; Aberle, K. K.; Janda, K. D.; Wilson, B. A. Tandem fluorescent proteins as enhanced FRET-based substrates for botulinum neurotoxin activity. *Toxicon* **2009**, *53* (4), 392–399.
- (21) Breidenbach, M. A.; Brunger, A. T. Substrate recognition strategy for botulinum neurotoxin serotype A. *Nature* **2004**, *432* (7019), 925–929.
- (22) Silvaggi, N. R.; Boldt, G. E.; Hixon, M. S.; Kennedy, J. P.; Tzipori, S.; Janda, K. D.; Allen, K. N. Structures of Clostridium botulinum Neurotoxin Serotype A Light Chain Complexed with Small-Molecule Inhibitors Highlight Active-Site Flexibility. *Chem. Biol.* **2007**, *14* (5), 533–542.
- (23) Crystallographic studies are ongoing and should provide more detailed binding information for these two unusual inhibitors.
- (24) DeLano, W. L. The PyMOL Molecular Graphics System 0.99; DeLano Scientific: Palo Alto, CA, USA, 2006.
- (25) Word, J. M.; Lovell, S. C.; Richardson, J. S.; Richardson, D. C. Asparagine and glutamine: using hydrogen atom contacts in the choice of side-chain amide orientation. *J. Mol. Biol.* **1999**, *285* (4), 1735–1747.
- (26) Hornak, V.; Abel, R.; Okur, A.; Strockbine, B.; Roitberg, A.; Simmerling, C. Comparison of multiple Amber force fields and development of improved protein backbone parameters. *Proteins: Struct., Funct., Bioinf.* **2006**, *65* (3), 712–725.
- (27) Case, D. A.; Darden, T. A.; Cheatham, T. E., III; Simmerling, C. L.; Wang, J.; Duke, R. E.; Luo, R.; Walker, R. C.; Zhang, W.; Merz, K. M.; Roberts, B.; Hayik, S.; Roitberg, A.; Seabra, G.; Kolossváry, I.; Wong, K. F.; Paesani, F.; Vanicek, J.; Liu, J.; Wu, X.; Brozell, S. R.; Steinbrecher, T.; Gohlke, H.; Cai, Q.; Ye, X.; Wang, J.; Hsieh, M.-J.; Hornak, V.; Cui, G.; Roe, D. R.; Mathews, D. H.; Seetin, M. G.; Sagui, C.; Babin, V.; Luchko, T.; Gusarov, S.; Kovalenko, A.; Kollman, P. A. AMBER 11; University of California, San Francisco, 2010.
- (28) Wang, J.; Wang, W.; Kollman, P. A.; Case, D. A. Automatic atom type and bond type perception in molecular mechanical calculations. *J. Mol. Graphics Modell.* **2006**, *25* (2), 247–260.
- (29) Granovsky, A. A. *Firefly*, 7.1.G. <http://classic.chem.msu.su/gran/firefly/index.html>, 1994.
- (30) Onufriev, A.; Bashford, D.; Case, D. A. Modification of the Generalized Born Model Suitable for Macromolecules. *J. Phys. Chem. B* **2000**, *104* (15), 3712–3720.
- (31) Onufriev, A.; Bashford, D.; Case, D. A. Exploring protein native states and large-scale conformational changes with a modified generalized born model. *Proteins* **2004**, *55* (2), 383–94.
- (32) Weiser, J.; Shenkin, P. S.; Still, W. C. Approximate atomic surfaces from linear combinations of pairwise overlaps (LCPO). *J. Comput. Chem.* **1999**, *20* (2), 217–230.
- (33) Roxas-Duncan, V.; Enyedy, I.; Montgomery, V. A.; Eccard, V. S.; Carrington, M. A.; Lai, H.; Gul, N.; Yang, D. C. H.; Smith, L. A. Identification and Biochemical Characterization of Small-Molecule Inhibitors of Clostridium botulinum Neurotoxin Serotype A. *Antimicrob. Agents Chemother.* **2009**, *53* (8), 3478–3486.
- (34) Ferrer-Montiel, A. V.; Canaves, J. M.; DasGupta, B. R.; Wilson, M. C.; Montal, M. Tyrosine Phosphorylation Modulates the Activity of Clostridial Neurotoxins. *J. Biol. Chem.* **1996**, *271* (31), 18322–18325.
- (35) Gul, N.; Smith, L. A.; Ahmed, S. A. Light Chain Separated from the Rest of the Type A Botulinum Neurotoxin Molecule Is the Most Catalytically Active Form. *PLoS ONE* **2010**, *5* (9), e12872.